

Original Study

Computed Tomographic Characteristics of Normal Lungs in Blue and Yellow Macaws (*Ara ararauna*)

Ieverton Cleiton Correia da Silva, Marília de Albuquerque Bonelli,
Ananda Santiago de Oliveira, José Anderson da Silva Rocha, Thaiza Helena Tavares Fernandes,
Tobias Schwarz, and Fabiano Séllos Costa

Abstract: Respiratory disease is common in psittacine birds; thus, having evidence-based methods to evaluate clinical cases is important for confirming a diagnosis. The purpose of this study was to describe the computed tomographic characteristics of the normal lung parenchyma of wild blue and yellow macaws (*Ara ararauna*), including measuring lung volume and normal radiographic attenuation of the lung parenchyma. Ten blue and yellow macaws from a wildlife center were used for this study. For computed tomography, transverse 1-mm slices were obtained, as well as multiplanar and 3-dimensional reconstructions for description of tomographic anatomy. Quantitative lung radiodensity was evaluated by regions of interest and via the histogram method. The lungs occupied the dorsal region of the coelomic cavity, with a triangular appearance on sagittal view, and were divided into left and right lungs. The lungs showed no lobulation. Mean attenuation values obtained were -727.19 ± 44.53 Hounsfield units by the histogram method and -722.19 ± 29.69 Hounsfield units by regions of interest. There was no significant difference ($P > 0.05$) between methods. Mean lung volume was 26 ± 6.03 cm³. The description of the normal computed tomography lung anatomy and density values of blue and yellow macaws are useful baseline data that can be applied to the diagnosis of respiratory diseases in this species.

Key words: lung diseases, blue and yellow macaw, radiodensity, computed tomography, avian, psittacine, *Ara ararauna*

INTRODUCTION

Psittacidae is a family of birds commonly raised in captivity and kept as exotic pets throughout the world. The blue and yellow macaw (*Ara ararauna*) is a popular species that is highly adaptable and has been successfully bred in captivity. In the wild, it can be found throughout South America and parts of Central America, from the northern region of Panama to the southern region of Argentina.¹ Due to widespread distribution and breeding success in captivity, removal of these birds from the wild for the pet trade has decreased over the past several

decades, and they are no longer listed in the International Union for Conservation of Nature list of threatened species.^{1,2}

Pulmonary diseases, such as pneumonia, are commonly seen in this species, especially in macaws raised in captivity because of inadequate care and feeding.³ Because this species is a prey species, these birds can mask signs of illness. Moreover, although a physical examination can provide insight into the health of a macaw, low-grade disease may be difficult to confirm. As such, information obtained from supplementary diagnostic tests has an added importance for early diagnosis of these diseases.⁴

Diagnostic imaging techniques have an important role in the clinical care of birds. There are a number of studies reporting normal anatomical characteristics in several animal species.⁵⁻⁷ However, there are few studies describing the use of computed tomography (CT) to evaluate the coelomic cavity of birds.^{4,8} The only study to mention blue and yellow macaws described the anatomical characteristics of the lungs;⁴ however, to the

From the Departamento de Medicina Veterinária, Universidade Federal Rural de Pernambuco, rua Dom Manuel de Medeiros, S/N, Recife, Pernambuco 52171-130, Brazil (da Silva, de Oliveira, Rocha, Costa); Ohio State University, 281 W Lane Ave, Columbus, OH 43210, USA (Bonelli); Centro Universitário Maurício de Nassau, rua Jonathas de Vasconcelos, 92, Recife, Pernambuco 51021-140, Brazil (Fernandes); and the Royal Dick School of Veterinary Studies, Roslin Midlothian EH25 9RG, UK (Schwarz).

Corresponding Author: Fabiano Séllos Costa, fabianoseillos@hotmail.com



Figure 1. Photograph demonstrating the positioning of a blue and yellow macaw (*Ara ararauna*) for a lung computed tomography scan. The macaw is positioned in ventral recumbency on a foam cradle.

authors' knowledge, there are no data available describing lung volume or radiographic attenuation of the lungs in this species.

The purpose of this study was to describe the normal CT anatomy, lung volume, and radiographic attenuation of the lung parenchyma of healthy wild blue and yellow macaws. The specific objectives of the study were to evaluate lung radiodensity by regions of interest (ROIs) and via the histogram method. The specific hypothesis being tested was that there would not be a difference between these methods.

MATERIALS AND METHODS

Ten blue and yellow adult macaws captured by the Wildlife Triage Center of Pernambuco (Brazil) between February and November 2019 were enrolled in this study. The macaws were captured by government agencies after entering residences, businesses, or other densely populated areas. The birds were kept under managed care at the Wildlife Triage Center of Pernambuco for 7 to 30 days while being evaluated for health issues; healthy macaws would be later released back into the wild. During the time they were in captivity, the macaws were kept in enclosures measuring approximately 10 m² and were provided with environmental enrichment, a balanced diet (77% extruded food [Megazoo Premium, Betim, Minas Gerais, Brazil], 5% seeds, and 18% fruit), and water ad libitum. Physical examinations, laboratory tests, and CT scans were performed prior to release into the wild to evaluate the health of

each macaw. Each bird was weighed during the physical examination, and the average weight of the macaws was 0.95 ± 0.05 kg. Sexing was not performed. Each bird had a hemogram and serum biochemistry assay performed; the biochemistries measured included alanine aminotransferase, aspartate aminotransferase, and alkaline phosphatase. All 10 macaws were considered healthy based on their physical examination results and blood values being within the accepted reference intervals for this species.³

The macaws were anesthetized for the CT scans. Anesthesia was induced in an induction box with 8% sevoflurane (1 mL/mL, Cristália, São Paulo, Brazil) and maintained with a face mask with sevoflurane at 2% in 1 L/minute oxygen to perform the CT exam. The macaws were then placed in ventral recumbency with a small foam cradle (Fig 1).

Computed tomography scans were performed with a single-slice CT scanner (Hi-Speed FXI, General Electric, Fairfield, CT, USA). The CT scanner was calibrated using the manufacturer's recommendations prior to the scans to ensure better standardization of the results. Transverse 1-mm thick helical images were obtained cranio-caudally with 1-mm slice interval, 0.8 pitch, 120 kV, and auto milliamperes, using a reconstruction algorithm for lung parenchyma.

Images were evaluated with a dedicated DICOM viewer (Horos version 3.3.5, Purview, Annapolis, MD, USA). To evaluate the images, multiplanar reconstructions and various windows were used according to the observer's preference. Evaluation of the anatomy of the

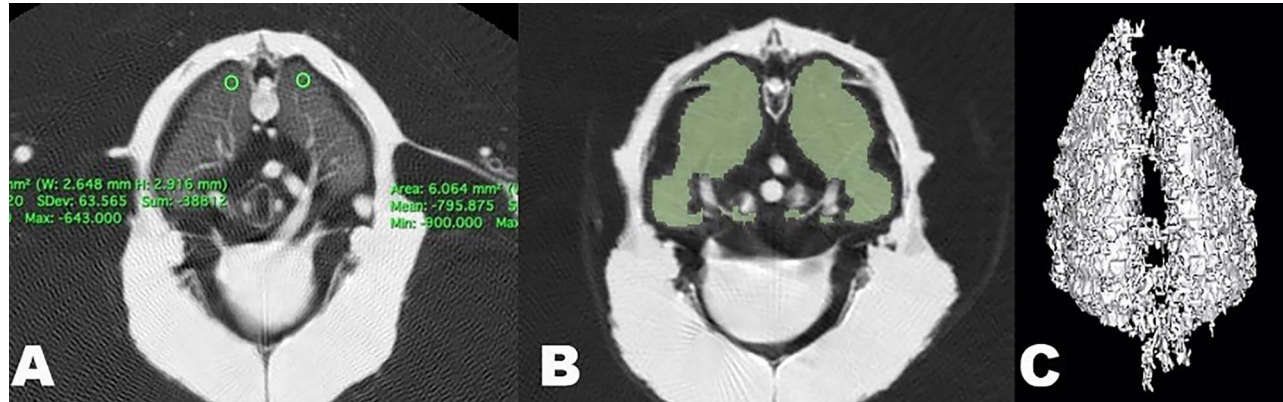


Figure 2. Transverse and volumetric reconstruction computed tomography images for blue and yellow macaws (*Ara ararauna*) demonstrating 2 methods for measuring mean radiographic attenuation of the lung parenchyma: (A) selection of regions of interest at the dorsolateral aspect of the lungs (green circles) and (B) selection of the lung parenchyma using the grow region tool (green area). Image (C) represents the volumetric reconstruction of the lung parenchyma.

respiratory system was based on anatomical references for other birds^{4,9} and described according to the CT findings. Radiographic attenuation values were measured in Hounsfield units by 2 distinct methods for quantitative analysis of lung parenchyma radiodensity: the ROI and histogram methods.

For the ROI method, transverse slices at the level of the caudal scapula were selected for each lung. An ROI with a diameter of 6 mm was then selected from the dorsolateral aspect of each lung, avoiding vascular structures and airways (Fig 2A). The size and form of the ROIs were identical in both lung lobes; this was ensured by using the copy and paste tool.¹⁰

For the histogram method, a radiographic attenuation interval between -1023 and -205 Hounsfield units was selected. The grow region tool, which measures air-filled spaces after selection of the area of interest, was then used to select the lung parenchyma (Fig 2B). Mean radiographic attenuation values for the lung parenchyma were then obtained from 3-dimensional reconstructions using this selected area (Fig 2C).⁵

Statistical analysis

The Shapiro-Wilk test was used to determine the normality of the data. Descriptive measurements obtained for the data were reported as mean \pm SD, median, and interquartile range (IQR). For comparison between the ROI and histogram methods, a paired Student *t* test and Pearson correlation coefficient were used. An $\alpha = 0.05$ was used to determine statistical significance. Statistical analyses were performed by a commercial software package (SPSS Statistics 23.0, IBM, Armonk, NY, USA).

RESULTS

On CT images, the lungs were observed to occupy the dorsal region of the coelomic cavity, with a triangular shape on sagittal images (Fig 3). Lungs were divided into left and right lobes and did not have lobulations. The costal arch region was observed to be in close contact with the lung surface, leaving impressions (sulci) on the lung surface and separating the lungs into compartments. The cranial margins of the lungs were located

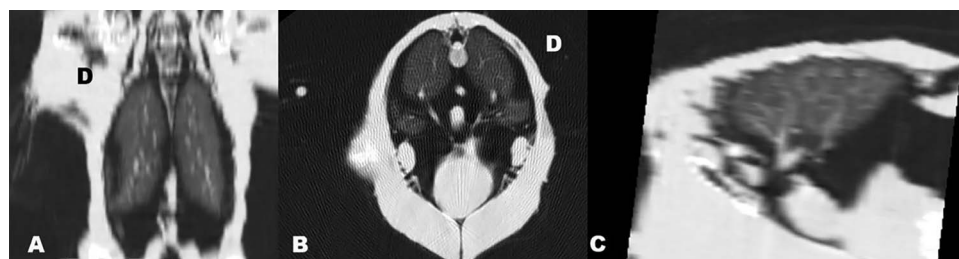


Figure 3. Transverse and multiplanar computed tomography reconstructions of the lung of blue and yellow macaws (*Ara ararauna*) used for anatomical description: (A) coronal reconstruction, (B) transverse view, and (C) sagittal reconstruction. Motion artifact in the image was due to the patient's breathing and breath holding, a technique that could have been used to control motion, was not used in this study.

Table 1. Descriptive statistics for the radiographic attenuation values for the lung parenchyma of 10 blue and yellow macaws (*Ara ararauna*) obtained by regions of interest and the histogram technique, as well as lung volume. Measures of radiographic attenuation are in Hounsfield units.

Evaluation method	Mean \pm SD	Median (IQR)
ROI—right lobe	-726.92 \pm 29	-723.40 (-760.66 to -707.68)
ROI—left lobe	-722.19 \pm 30	-721.34 (-752.87 to -694.89)
Histogram	-727.19 \pm 45	-737.15 (-756.67 to -691.15)
Lung volume, cm ³	26.00 \pm 6	25.54 (22.16 to 30.04)

Abbreviation: IQR, interquartile range; ROI, region of interest; SD, standard deviation.

at the level of the first ribs and the caudal margins extended slightly past the last rib. A hilum was present on the ventral surface of each lung lobe, where vascular structures and the main bronchus could be seen. Smaller bronchial structures (secondary bronchi) were also identified in 60% (6 of 10) of the macaws. The aorta, esophagus, and heart were observed ventral to the lungs. Cranial and caudal thoracic air sacs were located ventral to the lungs in all macaws.

Lung parenchyma radiodensity values obtained via the ROI and histogram methods, as well as lung volume, are displayed in Table 1. There were no significant differences ($P > 0.05$) between attenuation values obtained via ROIs or histogram. There was also no significant difference between right and left lungs by either method ($P > 0.05$). Significant positive correlations were observed between radiographic attenuation obtained via ROIs and via histogram, per lung lobe (right lobe, $r = 0.68$, $P = 0.031$; left lobe, $r = 0.733$, $P = 0.016$). Also, a significant negative correlation was observed between radiographic attenuation obtained via ROIs and lung volume for the left lung lobe ($r = -0.723$, $P = 0.023$) but not the right lobe ($r = -0.558$, $P = 0.093$).

DISCUSSION

This study documents the CT anatomy of the lungs of blue and yellow macaws, as well as the radiographic attenuation of the lung parenchyma and lung volume. To the authors' knowledge, this is the first use of histogram and lung volume analysis in blue and yellow macaws.

Pulmonary diseases are common in avian medicine, affecting various species of birds.^{4,11} In members of the Psittacidae family, fungal and bacterial lesions are reportedly prevalent.^{10,11} There are also reports of primary lung neoplasia and metastasis,¹²⁻¹⁴ in which a precise diagnosis or location is difficult to obtain via radiography due to the complexity of the avian respiratory system.¹⁵

The use of CT for diagnosing pulmonary disease in domestic animals, as well as in pet birds, is increasing.^{4,5,8,16,17} A primary advantage of CT over radiography is that it allows a 3-dimensional visualization of intrathoracic and intra abdominal structures. Specifically in birds, CT has been a valuable tool for the diagnosis of small lung lesions and defining the margins of larger tumors.^{12,16} Some studies support the use of CT for evaluation of the lung parenchyma in birds and the importance of associating a qualitative analysis of the lung parenchyma in various planes with densitometry of the lungs for diagnosing diseases such as pneumonia.^{8,9}

Macroscopically, bird lungs are located cranially and dorsally in the coelomic cavity. Dorsally, they are fixed to the vertebrae and ribs in a way that the ribs leave impressions on the lungs.¹⁸ These characteristics were clearly observed in all macaws evaluated in the present study.

In all the macaws imaged in the present study, 2 central vascular structures of similar caliber and a primary bronchial structure were identified. This was in line with previous descriptions in specimens from 3 species of the Psittacidae family raised as pets (blue and yellow macaws, grey parrots [*Psittacus erithacus*], and monk parakeets [*Myiopsitta monachus*]) where main bronchi and pulmonary arteries and veins were characterized by CT.⁴ Another report described the CT appearance of avian lungs as homogeneous structures similar to honeycombs, with each lobe having a central blood vessel and several secondary bronchi.¹⁹ In the present study, visualization of the secondary bronchi was only possible in some macaws, perhaps because macaws are smaller in size than the gyrfalcons (*Falco rusticolus*) in the previous description.¹⁹

Quantitative CT has been widely used as an adjunct in diagnosing changes to bony tissues and organs such as the liver and lungs in humans^{20,21} and companion animals.^{17,22} In exotic animals, there have also been reports of its use to evaluate lung parenchyma in foxes,⁵ snakes,⁷ tortoises,^{6,23} and birds, specifically whooping

cranes (*Grus americana*)¹⁰ and pet parrots.⁴ Mean radiographic attenuation for lung parenchyma of macaws in this study obtained via quantitative analysis by ROIs and the histogram technique was similar to that reported in the literature for avian lung parenchyma,¹⁹ specifically in blue and yellow macaws, grey parrots, and monk parakeets.⁴

The absence of a significant difference between the 2 quantitative methods used indicates either may be used for evaluation of the lung parenchyma; however, their individual usefulness may vary according to the type of disease being studied. The use of ROIs is widely employed for evaluation of liver and lung parenchyma,^{22,24} and evaluates the radiodensity of specific anatomical regions within the organs. This helps to facilitate the identification of focal changes in lung density, which can be useful in diagnosing diseases by detecting specific opacities such as aspergillosis granulomas.¹⁰ On the other hand, the histogram method evaluates the mean radiographic attenuation of the entire lung parenchyma. Histogram analysis of the lung parenchyma and lung volume has been used in humans,^{20,21} foxes,⁵ and tortoises,^{6,23} but there have been no previous reports of its use in birds.

It was not possible to determine the phase of the respiratory cycle during image acquisition because we used a face mask to deliver the anesthetic. Because avian lungs are considered static structures, they have a greater number of pulmonary capillaries and gas exchange can occur during both the inspiratory and expiratory phases, making them more efficient than mammalian lungs.¹¹ Lung volume on its own is therefore of less diagnostic importance in birds because there are few variations, and differentiating expiratory or inspiratory phases during the exam is of limited significance.¹⁹

The histogram method is useful for identifying changes in radiodensity of the lung parenchyma.¹⁹ A study performed in Humboldt penguins (*Spheniscus humboldti*) investigated lung density according to recumbency during the CT scan. Those authors found statistical differences between ventral, dorsal, and right lateral recumbencies, with higher lung density seen on ventral recumbency.¹⁵ Another study evaluating red-tailed hawks (*Buteo jamaicensis*) found similar results.²⁵ Based on these studies, this was the position adopted in the present study. Also, 3-dimensional analysis by the histogram method results in a better analysis of the lung parenchyma and can be a sensitive diagnostic tool for early detection of lesions.^{15,19}

Several lung diseases can cause changes to lung radiodensity, which in turn may be classified as focal or diffuse changes.^{12,21,23} Common changes found in birds

with lung diseases that result in interstitial accumulation of secretions tend to lead to higher lung radiodensity levels.^{10,26} Neoplastic lesions were also found to cause changes in conformation and density of lung parenchyma in the scarlet macaw (*Ara macao*).¹²

The present study has some inherent limitations for the use of these results as baseline values for radiographic attenuation. It is known that radiographic attenuation for a certain structure may vary between 7 and 56 Hounsfield units depending on kilovoltage peak, the material being evaluated, and the CT scanner used. Other variables, including kilovoltage peak, milliamperes, reconstruction algorithm, and slice thickness, can also affect the radiographic attenuation of a specific organ between patients under the same scanning technique.²² In the present study, interference from variables that are not inherent in the technique were considered low due to homogeneity of the sample population, calibration of the CT scanner prior to each exam, and the use of the same technique for all the scans. However, it is appropriate to keep the aforementioned limitations in mind when using these results for any future comparisons. Another limitation of the study was the presence of movement artifacts. Although respiratory movements caused some minor artifacts, these did not significantly interfere with the evaluation of the parameters assessed in this study. Future studies should consider using a breath holding technique to minimize respiratory movement artifacts.

This study provides an anatomical description with quantitative measurements of attenuation and volume of the lungs by CT in wild blue and yellow macaws. Normal quantitative lung density values were obtained by ROIs and the histogram method. Both methods were viable for the evaluation of lung radiodensity and show potential for their use in the early diagnosis of lung diseases of macaws, as well as for use with serial evaluations in patients with chronic diseases. The present study can also serve as a basis for future studies on lung patterns observed in various respiratory diseases in blue and yellow macaws.

REFERENCES

1. Jordan R, Moore M. *A Guide To . . . Macaws as Pet and Aviary Birds*. 2nd ed. ABK Publications; 2015.
2. BirdLife International. *Ara ararauna*. The IUCN Red List of Threatened Species. Aug 09, 2018. <https://www.iucnredlist.org/ja/species/22685539/131917270> Accessed June 01, 2024.
3. Grespan A, Freitas TR. Psittaciformes (Araras, Papagaios, Periquitos, Calopsitas e Cacatuas). In: Cubas Z, Silva J, Catão-dias J, eds. *Tratado de Animais Selvagens*. Vol 1. 2nd ed. Roca; 2014:550–589.

4. Veladiano IA, Banzato T, Bellini L, et al. Normal computed tomographic features and reference values for the coelomic cavity in pet parrots. *BMC Vet Res.* 2016;12:1–9.
5. McEvoy F, Buelund L, Strathe A, et al. Quantitative computed tomography evaluation of pulmonary disease. *Vet Radiol Ultrasound.* 2009;50:47–51.
6. Silva ICC, Bonelli MA, Rameh-de-Albuquerque LC, et al. Computed tomography of the lungs of healthy captive red-footed tortoises (*Chelonoidis carbonaria*). *J Exot Pet Med.* 2020;34:27–31.
7. Pees M, Kiefer I, Thielebein J, et al. Computed tomography of the lung of healthy snakes of the species *Python regius*, *Boa constrictor*, *Python reticulatus*, *Morelia viridis*, *Epicrates cenchria* and *Morelia spilota*. *Vet Radiol Ultrasound.* 2009;50:487–491.
8. Gumpenberger M, Henninger W. The use of computed tomography in avian and reptile medicine. *Sem Avian Exot Pet Med.* 2001;10:174–180.
9. Gumpenberger M. Avian. In: *Veterinary Computed Tomography*. 1st ed. Wiley-Blackwell; 2011:517–532.
10. Schwartz T, Kelley C, Pinkerton ME, et al. Computed tomography anatomy and characteristics of respiratory aspergillosis in juvenile whooping cranes. *Vet Radiol Ultrasound.* 2016;57:16–23.
11. Tully T Jr, Harrison G. Pneumology. In: Ritchie B, Harrison G, Harrison L, eds. *Avian Medicine: Principle and Application*. Wingers Publishing, Lake Worth, FL; 1994:556–581.
12. Marinkovich M, Quesenberry K, Donovan TA, et al. Use of standing computed tomography for the diagnosis of a primary respiratory adenocarcinoma in a scarlet macaw (*Ara macao*). *J Exot Pet Med.* 2017;26:101–107.
13. Fredholm DV, Carpenter JW, Shumacher LL, et al. Pulmonary adenocarcinoma with osseous metastasis and secondary paresis in a blue and gold macaw (*Ara ararauna*). *J Zoo Wildl Med.* 2012;43:909–913.
14. Lamb S, Reavill D, Wojcieszyn J, et al. Osteosarcoma of the tibiotarsus with possible pulmonary metastasis in a ring-necked dove (*Streptopelia risoria*). *J Avian Med Surg.* 2014;28:50–56.
15. Nevitt BN, Langan JN, Adkesson MJ, et al. Comparison of air sac volume, lung volume, and lung densities determined by use of computed tomography in conscious and anesthetized Humboldt penguins (*Spheniscus humboldti*) positioned in ventral, dorsal, and right lateral recumbency. *Am J Vet Res.* 2014;75:739–745.
16. Newell SM, Roberts GD, Bennett A. Imaging techniques for avian lower respiratory diseases. *Sem Avian Exot Pet Med.* 1997;6:180–186.
17. Dennler M, Makara M, Kranjc A, et al. Thoracic computed tomography findings in dogs experimentally infected with *Angiostrongylus vasorum*. *Vet Radiol Ultrasound.* 2011;52:289–294.
18. König H, Navarro M, Zengerling G, et al. Respiratory system (apparatus respiratorius). In: König H, Korb R, Liebich H, eds. *Avian Anatomy*. 2nd ed. 5M Publishing; 2016:118–130.
19. Krautwald-Junghanns M, Pees M. Computed tomography (CT). In: Krautwald-Junghanns M, Pees M, Reese S, et al, eds. *Diagnostic Imaging of Exotic Pets*. Schlütersche; 2011:54–63.
20. Sumikawa H, Johkoh T, Yamamoto S, et al. Quantitative analysis for computed tomography findings of various diffuse lung diseases using volume histogram analysis. *J Comput Assist Tomogr.* 2006;30:244–249.
21. Coxson HO. Sources of variation in quantitative computed tomography of the lung. *J Thorac Imaging.* 2013;28:272–279.
22. Lam R, Niessen SJ, Lamb CR. X-ray attenuation of the liver and kidney in cats considered at varying risk of hepatic lipidosis. *Vet Radiol Ultrasound.* 2014;55:141–146.
23. Lim CK, Kirberger RM, Lane EP, et al. Computed tomography imaging of a leopard tortoise (*Geochelone pardalis pardalis*) with confirmed pulmonary fibrosis: a case report. *Acta Vet Scand.* 2013;55:35.
24. Bonelli MA, Oliveira DC, Costa LAVS, et al. Quantitative computed tomography of the liver in juvenile green sea turtles (*Chelonia mydas*). *J Zoo Wildl Med.* 2013;44:310–314.
25. Malka S, Hawkins MG, Jones JH, et al. Effect of body position on respiratory system volumes in anesthetized red-tailed hawks (*Buteo jamaicensis*) as measured via computed tomography. *Am J Vet Res.* 2009;70:1155–1160.
26. Akira M, Toyokawa K, Inoue Y, et al. Quantitative CT in chronic obstructive pulmonary disease: inspiratory and expiratory assessment. *Am J Roentgenol.* 2009;192:267–272.